

## Cloud Retrieval Using Infrared Sounder Data: Error Analysis

BRUCE A. WIELICKI<sup>1</sup> AND JAMES A. COAKLEY, JR.

National Center for Atmospheric Research,<sup>2</sup> Boulder, CO 80307

(Manuscript received 22 July, 1980, in final form 21 November 1980)

### ABSTRACT

An error analysis is presented for cloud-top pressure and cloud-amount retrieval using infrared sounder data. Rms and bias errors are determined for instrument noise (typical of the HIRS-2 instrument on TIROS-N) and for uncertainties in the temperature profiles and water vapor profiles used to estimate clear-sky radiances. Errors are determined for a range of test cloud amounts (0.1–1.0) and cloud-top pressures (920–100 mb). Rms errors vary by an order of magnitude depending on the cloud height and cloud amount within the satellite's field of view. Large bias errors are found for low-altitude clouds. These bias errors are shown to result from physical constraints placed on retrieved cloud properties, i.e., cloud amounts between 0.0 and 1.0 and cloud-top pressures between the ground and tropopause levels. Middle-level and high-level clouds (above 3–4 km) are retrieved with low bias and rms errors. For instrument noise the 4.3  $\mu\text{m}$  channels provide the smallest errors. For temperature profile and water vapor profile uncertainties the 15  $\mu\text{m}$  channels generally give smaller errors. Errors due to rms temperature profile uncertainties of 2.0°C are found to be larger than errors due to instrument noise, independent of the sounding channels used.

### 1. Introduction

Satellite observations could provide global coverage of cloud properties such as cloud-top height and temperature, fractional cloud cover, and perhaps cloud reflectivity and emissivity. Such data are essential for the inclusion of cloud parameterizations in realistic models of the earth's climate (Schneider, 1972; Cess, 1974; Stephens and Webster, 1979). The development and assessment of cloud models, however, necessitates an understanding of the uncertainties, both random and biased, inherent in satellite-observed cloud properties. Here we provide a theoretical evaluation of one class of satellite-based cloud retrievals: those derived from observations made with infrared sounding radiometers.

The infrared sounder retrieval methods require the fewest *a priori* assumptions about the spatial scales and radiative properties of the clouds. In particular, cloud fractional coverage and cloud emissivity can be less than 1.0. This freedom is important for the retrieval of cirrus clouds. We consider the methods described by Chahine (1975) and by Smith and Platt (1978). The method used by Smith and Platt was initially presented by Smith *et al.* (1970). These procedures use a combination of radiances in the 15  $\mu\text{m}$  CO<sub>2</sub> band, the 4.3  $\mu\text{m}$  CO<sub>2</sub>/N<sub>2</sub>O band,

and the 11  $\mu\text{m}$  window along with knowledge of temperature and humidity profiles to determine cloud top altitude and fractional cloud cover. Retrieval errors caused by instrument noise and uncertainties in temperature and humidity profiles are assessed.

### 2. Satellite radiances

For fields of view (FOV's) free of clouds, the clear-sky radiance  $I_{cs}(\nu)$  at wavenumber  $\nu$  measured by the satellite is given by

$$I_{cs}(\nu) = B(\nu, T_g)\tau(\nu, P_g) - \int_0^{P_g} B(\nu, T(P)) \frac{d\tau(\nu, P)}{d \ln P} d \ln P, \quad (1)$$

where  $B(\nu, T)$  is the Planck radiance at wavenumber  $\nu$  and temperature  $T$ ,  $\tau(\nu, P)$  is the transmission between atmospheric pressure level  $P$  and the satellite (at pressure  $P = 0$ ), and subscript  $g$  indicates ground level. In (1) the surface is assumed to be black (i.e., its emissivity is 1).

For completely overcast FOV's the radiance is given by

$$I_o(\nu) = B(\nu, T_c)\tau(\nu, P_c) - \int_0^{P_c} B(\nu, T(P)) \frac{d\tau(\nu, P)}{d \ln P} d \ln P. \quad (2)$$

In (2) the clouds are assumed to be black. For non-black clouds the reflectivity is assumed to be negligible so that the emissivity  $\epsilon(\nu)$  and transmissivity

<sup>1</sup> Present affiliation: NASA Langley Research Center, Hampton, VA 23665.

<sup>2</sup> The National Center for Atmospheric Research is sponsored by the National Science Foundation.

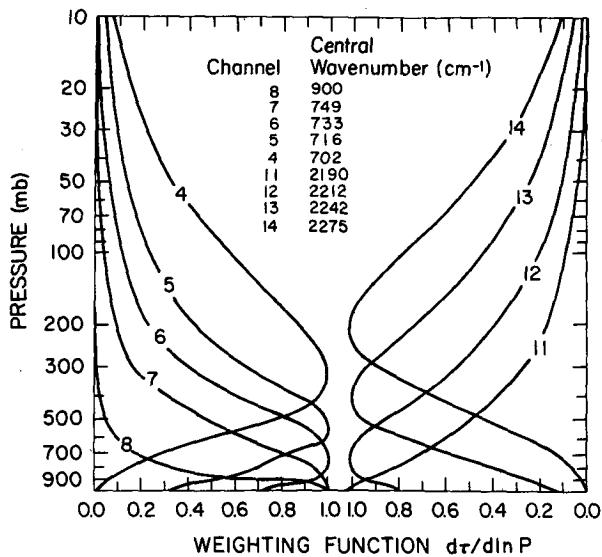


FIG. 1. Normalized weighting functions ( $d\tau/d \ln P$ ) for the HIRS-1 channels used in this study (midlatitude climatological profile).

$\tau(\nu)$  are related by  $\epsilon(\nu) + \tau(\nu) = 1$ . As a result, fractional coverage  $A_c$  by non-black clouds within the satellite field of view is equivalent to fractional coverage  $\epsilon(\nu)A_c$  by a black cloud. Satellite radiances for partially cloud-filled fields of view are thus given by

$$I(\nu) = I_{cs}(\nu) + \epsilon(\nu)A_c[I_0(\nu) - I_{cs}(\nu)]. \quad (3)$$

In this study the transmission functions  $\tau(\nu, P)$  used to calculate the radiances are for the HIRS-1 (High Resolution Infrared Sounder) instrument that flew on Nimbus 6. The transmission function computer code was provided by H. M. Woolf (private communication, 1978). The transmission functions include absorption by well-mixed gases, absorption by water vapor (including the water vapor continuum), and the effect of varying atmospheric temperature.

The HIRS-1 instrument measured radiances at 16 infrared channels. It had a subsatellite ground resolution of  $\sim 25$  km. The channels in the 4.3, 11 and 15  $\mu\text{m}$  bands used in this study are essentially the same as those in the HIRS-2 instrument of TIROS-N. The HIRS-2 instrument will be flown on NOAA operational satellites throughout the 1980's.

The weighting functions ( $d\tau/d \ln P$ ) for the channels are shown in Fig. 1 for a climatological average midlatitude profile taken from Fels and Schwarzkopf (1975). These functions vary slightly with changing temperature and water vapor profiles. Channels 4–7 are within the 15- $\mu\text{m}$   $\text{CO}_2$  band, 11–14 in the 4.3  $\mu\text{m}$   $\text{N}_2\text{O}/\text{CO}_2$  band, and 8 in the 11  $\mu\text{m}$  window. Forty pressure levels between 1000 and 0.2 mb are used to calculate by trapezoid rule the integrals in

(1) and (2). The levels used below 100 mb are 1000, 920, 850, 700, 600, 500, 400, 350, 300, 250, 200, 175, 150, 125 and 100 mb. For interpolation to model levels, temperature and the logarithm of water vapor mixing ratio are assumed linear in  $\ln P$ . The levels also serve to locate the tops of clouds as described in the next section.

### 3. Cloud-property retrieval

Let us consider the use of (1) through (3) to determine cloud pressure and amount within a single FOV. Assuming knowledge of the temperature and water vapor profile, we may calculate the Planck function and transmission functions needed to obtain the clear-sky radiance from (1). The overcast radiance in (2) becomes a function of  $P_c$  only. From (3) we obtain the change in measured radiance at wavenumber  $\nu^i$  due to the presence of cloud. This change is given by

$$\Delta I_{\text{cld}}^i = I^i - I_{cs}^i = \epsilon^i A_c [I_0^i(P_c) - I_{cs}^i], \quad (4)$$

where the superscript indicates channel wavenumber dependence. Using radiance measurements from  $N$  channels, we obtain a set of  $N$  equations for  $N + 2$  unknowns:  $A_c$ ,  $P_c$  and  $N$  emissivities. One approach to solving this system of equations is to assume black clouds ( $\epsilon^i = 1.0$ ). Although this assumption may be valid for low clouds, cirrus clouds commonly exhibit spectral emissivities  $\leq 0.5$  (Platt and Dilley, 1979). A more general approach selects channels for which we may assume  $\epsilon^i = \epsilon^j$  for a wide range of cloud types. This approach requires channels closely spaced in wavenumber. Channels on the HIRS instrument within the 15  $\mu\text{m}$  band or within the 4.3  $\mu\text{m}$  band could be used.

Several techniques have been proposed for the determination of cloud pressure and amount from the system of equations represented by (4). These techniques fall naturally into two categories and here we consider a typical example from each category.

Smith and Woolf (1976), McCleese and Wilson (1976) and Smith and Platt (1978) have each considered the technique which we shall refer to as the radiance ratioing method. For this method we consider the function given by

$$G^{ij}(P_c) = \frac{I^i - I_{cs}^i}{I^j - I_{cs}^j} = \frac{\Delta I_{\text{cld}}^i}{\Delta I_{\text{cld}}^j}, \quad (5)$$

i.e.,  $G(P_c)$  is the ratio of the cloud effect in two channels. With (4), Eq. (5) becomes

$$G^{ij}(P_c) = \frac{\epsilon^i [I_0^i(P_c) - I_{cs}^i]}{\epsilon^j [I_0^j(P_c) - I_{cs}^j]}. \quad (6)$$

We choose channels such that  $\epsilon^i = \epsilon^j$ . For a specified temperature and water vapor profile, we cal-

culate  $G^{ij}(P_c)$  from (6). Then we determine  $P_c$  from the value of  $G^{ij}$  obtained from (5) when measured radiances are used. Once  $P_c$  is determined, the lowest sounding channel is used with (3) to determine the effective cloud amount. The lowest sounding channel provides the largest cloud signal  $\Delta I_{\text{clid}}$ .

McCleese and Wilson (1976) pointed out that changes in mean profile temperature or lapse rate have little effect on  $G^{ij}(P_c)$ . Fig. 2 shows  $G^{ij}(P_c)$  for three climatological profiles taken from Fels and Schwarzkopf (1975). The two lowest 15  $\mu\text{m}$  sounding channels (6, 7) are used. The tropical and mid-latitude results are very similar up to the midlatitude tropopause. (For isothermal conditions  $G^{ij}$  is constant.) The climatological polar profile contains a large surface inversion. Because temperatures below 750 mb are warmer than the surface temperatures, clouds below 750 mb will cause cloudy radiances to exceed clear-sky radiances. As cloud-top temperature approaches ground temperature,  $\Delta I_{\text{clid}} \rightarrow 0.0$  and  $G^{ij}$  tends to  $\pm\infty$  as seen in Fig. 2. In view of the variability of temperature inversions in polar regions, we concentrate the present analysis on midlatitude and tropical conditions.

The performance of the ratioing method depends on the channels used. For channels that sound levels of the atmosphere above the cloud, Eqs. (1) and (2) show that  $I_b^i \approx I_{cs}^i$ , i.e., little cloud information is obtained. Thus, channels sounding the lower atmospheric levels are preferred. To satisfy  $\epsilon^i \approx \epsilon^j$ , channels also should be closely spaced in wavenumber. Finally, since the Planck functions for two closely spaced channels are nearly the same, the weighting functions for the two channels must be different in order to avoid redundant information ( $I^i \approx I^j$ ).

Turning now to the second retrieval method, Chahine (1975) proposed a solution based on the minimization of the rms difference between calculated and observed radiances. A knowledge of temperature profile and weighting functions is assumed. Clear-sky radiances for the  $N$  channels used are calculated from (1). A trial cloud pressure is chosen and the  $I_b^i$  are determined from (2). Using the channel whose weighting function peaks lowest in the atmosphere, an effective cloud amount ( $\epsilon A_c$ ) is determined from (3). Assuming the same emissivity in all  $N$  channels, the remaining radiances  $\hat{I}^i$  are calculated using  $P_c$  and  $\epsilon A_c$  in (2) and (3). The rms radiance difference is defined by

$$R(P_c, \epsilon A_c) = \left\{ \sum_i [\tilde{I}^i - \hat{I}^i(P_c, \epsilon A_c)]^2 \right\}^{1/2}. \quad (7)$$

where a tilde indicates measured radiances and a caret indicates calculated radiances.<sup>3</sup>

<sup>3</sup> Chahine (1975) minimized  $(\tilde{I}^i - \hat{I}^i)/\tilde{I}^i$ ; however, this quantity overemphasizes the higher (altitude) sounding channels which exhibit a smaller cloud signal  $\Delta I_{\text{clid}}$ . The radiance difference in (7)

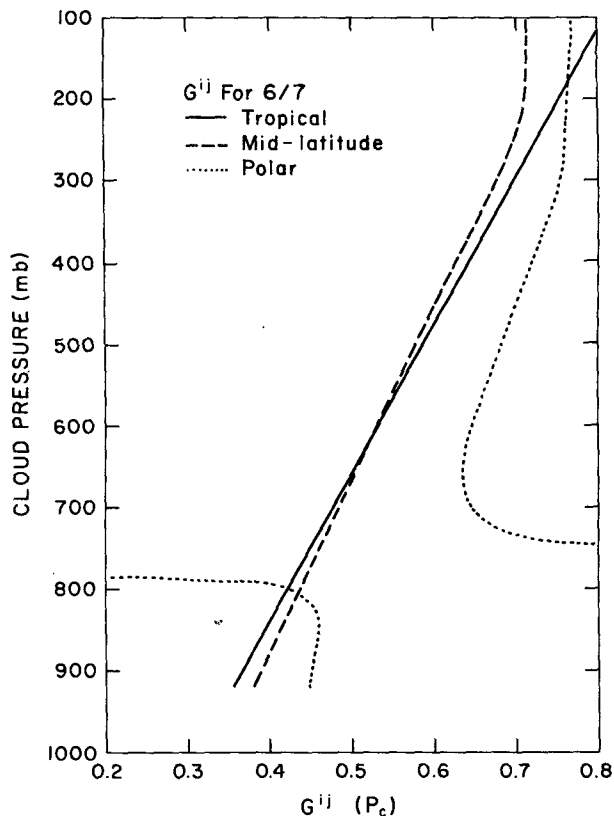


FIG. 2. The cloud pressure functional  $G^{ij}(P_c)$  shown for channel combination 6/7 using tropical, midlatitude and polar climatological profiles.

For solutions using two channels, the Chahine method is mathematically equivalent to the radiance ratioing method, provided  $\hat{A}_c < 1.0$ . Cases for which the retrieved  $\hat{A}_c > 1.0$  will be considered below. The primary use of the Chahine method will be to assess the effect of using more than two tropospheric sounding channels within either the 4.3 or 15  $\mu\text{m}$  bands.

The error analyses that follow were performed for a variety of channel combinations  $i/j$  for the HIRS-1 instrument. For simplicity of discussion, "black" clouds were used in all cases. Errors for non-black clouds are equivalent to the errors for effective black cloud amount  $\epsilon A_c$ . The smallest errors were obtained for 6/7 in the 15  $\mu\text{m}$  region and for 12/11 in the 4.3  $\mu\text{m}$  region. The combination 7/8 (the lowest sounding 15  $\mu\text{m}$  channel and the 11  $\mu\text{m}$  window channel) also gave low errors, but these channels are widely separated in wavenumber and thus could give poor results for non-black clouds. Nevertheless, this combination has been used by

is used in this study.  $R$  is calculated for a predetermined set of cloud pressure values between the surface and the tropopause. We choose the value of  $P_c$  and subsequent  $\epsilon A_c$  that lead to the smallest  $R$ .

Smith and Platt (1978) to retrieve properties of clouds below 500 mb. Results using the above two-channel combinations are presented for the radiance ratioing method. In addition, Chahine's method is applied to all tropospheric 15  $\mu\text{m}$  channels and separately to all 4.3  $\mu\text{m}$  tropospheric channels. Although all error analyses were performed for both tropical and midlatitude conditions, we present the midlatitude results. The differences between tropical and midlatitude errors ranged from 5 to 25% of the error reported here, varying in sign and magnitude as a function of cloud height, channel combination and error source. These differences were judged insufficient to warrant separate discussion.

#### 4. Errors due to instrument noise

##### a. Cloud-pressure rms errors

To estimate the errors due to instrument noise, we assume exact knowledge of the temperature and humidity profiles and, thereby, an exact knowledge of  $I_{cs}$ ,  $I_0(P_c)$  and  $G(P_c)$ : "Measured" radiances are then simulated for a range of 10 cloud amounts (0.1–1.0), 12 cloud-top pressures (920–100 mb) and two climatological mean profiles (tropical and midlatitude). After random instrument noise is added to the radiances, cloud amounts and pressures are retrieved. For each cloud amount and pressure combinations, 200 samples are constructed in order to investigate the statistical properties of the retrieved quantities. Instrument noise is taken to be Gaussian with zero mean and a standard deviation of 0.22  $\text{mW m}^{-2} \text{sr}^{-1} \text{cm}$  for the 15  $\mu\text{m}$  channels, 0.002  $\text{mW m}^{-2} \text{sr}^{-1} \text{cm}$  for the 4.3  $\mu\text{m}$  channels and 0.11  $\text{mW m}^{-2} \text{sr}^{-1} \text{cm}$  for the 11  $\mu\text{m}$  channel. These quantities are the noise levels specified for the HIRS-2 instrument on TIROS-N (Schwalb, 1978).<sup>4</sup>

Figs. 3a–3c show rms error in  $P_c$  (mb) obtained by applying the radiance-ratioing method to channel combinations: 6/7, 7/8 and 12/11. Data giving a measured  $\tilde{G}^{ij} < G$  (920 mb) were taken to indicate cloud-free FOV's. Data giving a  $\tilde{G}^{ij} > G$  (tropopause) were taken to indicate clouds at the tropopause.  $\tilde{A}_c < 0.0$  indicates cloud-free FOV's and  $\tilde{A}_c > 1.0$  is truncated to  $\tilde{A}_c = 1.0$ . As  $P_c \rightarrow 1000$  mb and as  $A_c \rightarrow 0$ , the cloud signal  $\Delta I_{\text{cl}}$  given by (4) becomes comparable to the instrument noise and the large errors shown in the figures result. Fig. 4 compares instrument noise to the overcast cloud signal,  $[I_{cs} - I_0(P_c)]$ . From Fig. 4 we would expect 12/11 to give the smallest errors, followed by 7/8 and 6/7. This expectation is confirmed by the cloud pressure errors in Fig. 3.

We now apply Chahine's cloud retrieval method in the presence of instrument noise. Test cloud

pressures are chosen every 25 mb between 1000 and 100 mb. Boundary conditions are similar to those for the radiance-ratioing method. Data giving cloud pressures below 925 mb are taken to indicate clear conditions. Data giving cloud pressures above the tropopause are taken to indicate cloud cover at the tropopause. Cloud-amount limitations are also the same. As expected, the Chahine technique gives the same rms errors when applied to the two-channel combinations shown above. If we add channels 5 and 4 to 6/7, rms  $P_c$  errors increase by a few percent for low clouds ( $P_c \geq 600$  mb). For clouds above 600 mb the 4-channel solution continually improves. For 200 mb clouds the added channels give 50% lower rms errors. Adding channels 13 and 14 to 12/11 produces similar effects. As stated earlier, the upper level sounding channels offer little information about low-level cloudiness.

##### b. Cloud-pressure bias errors

The cloud-pressure rms errors shown in the previous section are variations of retrieved cloud values about the *retrieved* mean cloud pressure or amount. Bias error, the difference between the actual mean and retrieved mean cloud value, must also be considered. The primary source of bias is the limiting of cloud amount to the range (0.0, 1.0) and cloud-top pressure to the range ( $P_{\text{ground}}$ ,  $P_{\text{tropopause}}$ ). Fig. 5a shows cloud pressure bias errors (midlatitude climatological profile) for 6/7 obtained by using the radiance-ratioing method. Clouds near the tropopause are biased low, and clouds near the ground are biased high. To test whether these biases are due to the nonlinear physical constraints placed on the retrieved cloud-top pressure, we develop a statistical model for retrieval error.

Consider the measured  $\tilde{G}^{ij}$  for cloud amount  $A_c$  and cloud-top pressure  $P_c$  when instrument noise  $\delta I^i$  and  $\delta I^j$  are present. From (4) and (5),  $\tilde{G}^{ij}$  is given by

$$\begin{aligned} \tilde{G}^{ij} &= G^{ij}(P_c) + \delta G^{ij} \\ &= \frac{A_c [I_{cs}^i - I_0^i(P_c)] + \delta I^i}{A_c [I_{cs}^j - I_0^j(P_c)] + \delta I^j}, \end{aligned} \quad (8)$$

where the estimated or measured value of a variable  $x$  is denoted by  $\tilde{x}$  and contains error  $\delta x$  (i.e.,  $\tilde{x} = x + \delta x$ ). For  $\delta I^m \ll [I_{cs}^m - I_0^m(P_c)]$ , the right-hand side of (8) is well represented by a linear expansion in  $\delta I^i$  and  $\delta I^j$ . Expanding the right-hand side of (8) and using (6) to eliminate  $G^{ij}(P_c)$  from the left-hand side of (8), we obtain an approximation for the error  $\delta G^{ij}$ :

$$\delta G^{ij} = \frac{1}{A_c [I_{cs}^j - I_0^j(P_c)]} [\delta I^i - G^{ij}(P_c) \delta I^j]. \quad (9)$$

Because the variance of the sum of two normally

<sup>4</sup> Schwalb, A., 1978: The TIROS-N/NOAA A-G Satellite Series. NOAA Tech. Memo., NESS 95, 75 pp.

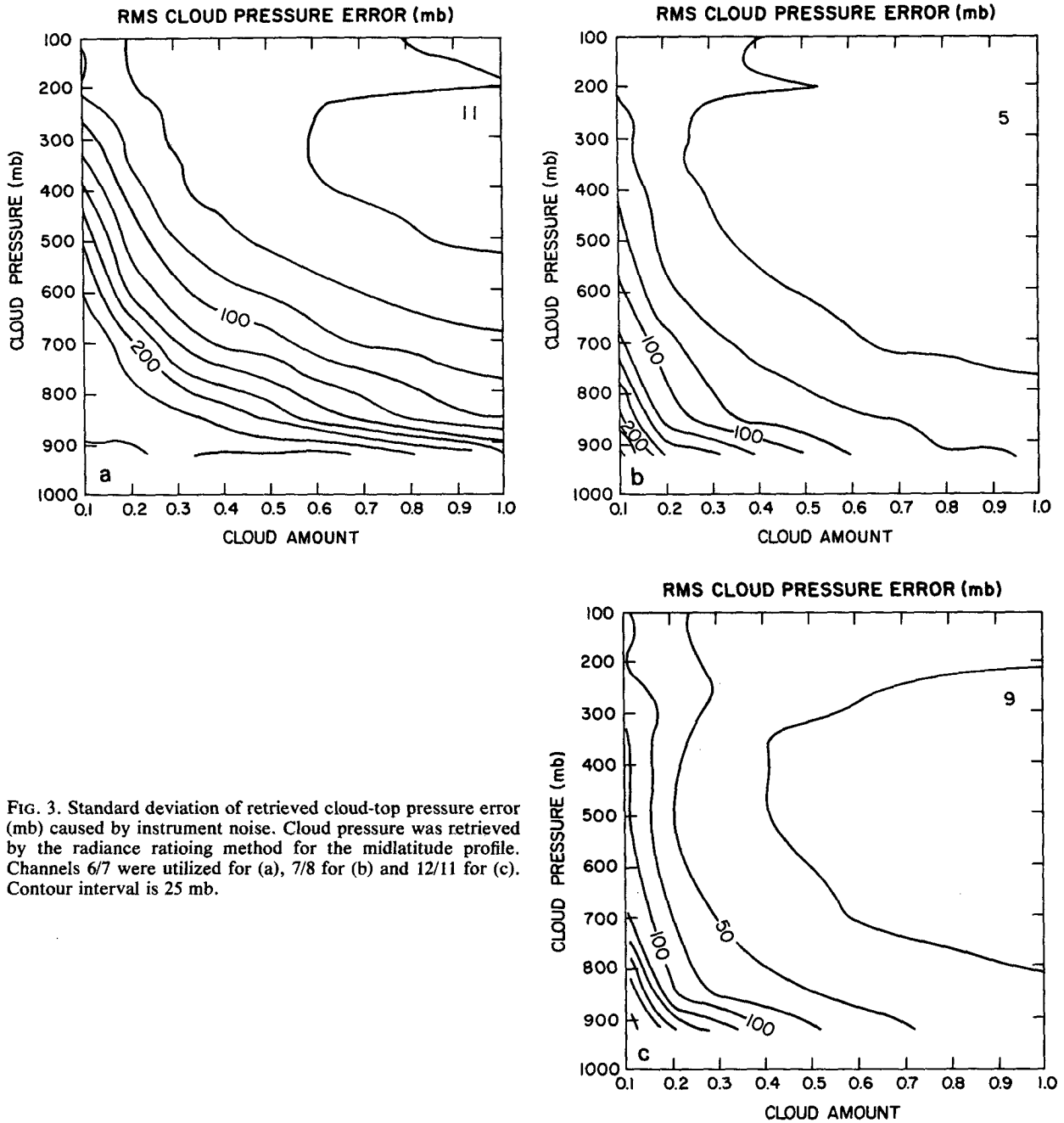


FIG. 3. Standard deviation of retrieved cloud-top pressure error (mb) caused by instrument noise. Cloud pressure was retrieved by the radiance ratioing method for the midlatitude profile. Channels 6/7 were utilized for (a), 7/8 for (b) and 12/11 for (c). Contour interval is 25 mb.

distributed variables is the sum of the individual variances, we can obtain from (9) an estimate of the standard deviation of the error in  $G^{ij}(P_c)$ . The standard deviation is given by

$$\sigma_G(P_c, A_c) = \frac{\{(\sigma_i^j)^2 + [G^{ij}(P_c)]^2(\sigma_j^i)^2\}^{1/2}}{A_c[I_{cs}^j - I_0^j(P_c)]}, \quad (10)$$

where  $\sigma_X(Y)$  denotes the standard deviation of variable  $X$  given some fixed parameter  $Y$ . We note that the standard deviation tends to infinity as either  $A_c \rightarrow 0$  or  $P_c \rightarrow P_g$ . We can now obtain cloud pres-

sure uncertainty by the transformation

$$\sigma_P(P_c, A_c) = \frac{1}{2} \{ P_c [G^{ij}(P_c) + \sigma_G(P_c, A_c)] - P_c [G^{ij}(P_c) - \sigma_G(P_c, A_c)] \}, \quad (11)$$

using Fig. 2 to obtain  $P_c(G^{ij})$ . For  $G^{ij} \pm \sigma_G$  outside the normal range of values for  $G^{ij}$ , we linearly extrapolate the endpoints in Fig. 2, i.e.,

$$\sigma_P(P_c, A_c) = \frac{\sigma_G(P_c, A_c)(920 \text{ mb} - 100 \text{ mb})}{[G(100 \text{ mb}) - G(920 \text{ mb})]}. \quad (12)$$

We now have an estimate of the cloud-pressure rms errors which would occur in the absence of physical limits on cloud height. Fig. 6 shows an idealized probability distribution for retrieved cloud height for clouds at level  $P_c$ . In the present retrieval scheme all data giving  $\bar{P}_c > 920$  mb are set to clear-

sky conditions and data giving  $\bar{P}_c < P$  (tropopause) are set to level PTROP. By assuming a Gaussian distribution for cloud-pressure errors in the absence of constraints, we calculate the second moment of the statistical distribution in the presence of boundaries as

$$Y2(P_c, A_c) = \frac{1}{\sigma\sqrt{2\pi}} \left[ \int_{PTROP}^{920} P^2 f(P) dP + PTROP^2 \int_{-\infty}^{PTROP} f(P) dP \right] \quad (13)$$

$$\left[ 1 - \frac{1}{\sigma\sqrt{2\pi}} \int_{920}^{\infty} f(P) dP \right]$$

where  $\sigma = \sigma_P(P_c, A_c)$  from (11) and  $f(P) = \exp[-(P - P_c)^2/2\sigma^2]$ , the Gaussian probability density function for the retrieved cloud pressure  $P = P_c$  and actual cloud pressure  $P_c$ . When clear conditions are indicated ( $\bar{P}_c > 920$  mb) the moment integral is set to

zero, i.e., there is no contribution to cloud statistics; the probabilities are normalized to the fraction of cloudy FOV's retrieved. The bias error (first moment) is given by

$$Y1(P_c, A_c) = \frac{1}{\sigma\sqrt{2\pi}} \left[ \int_{PTROP}^{920} P f(P) dP + PTROP \int_{-\infty}^{PTROP} f(P) dP \right] \quad (14)$$

$$\left[ 1 - \frac{1}{\sigma\sqrt{2\pi}} \int_{920}^{\infty} f(P) dP \right]$$

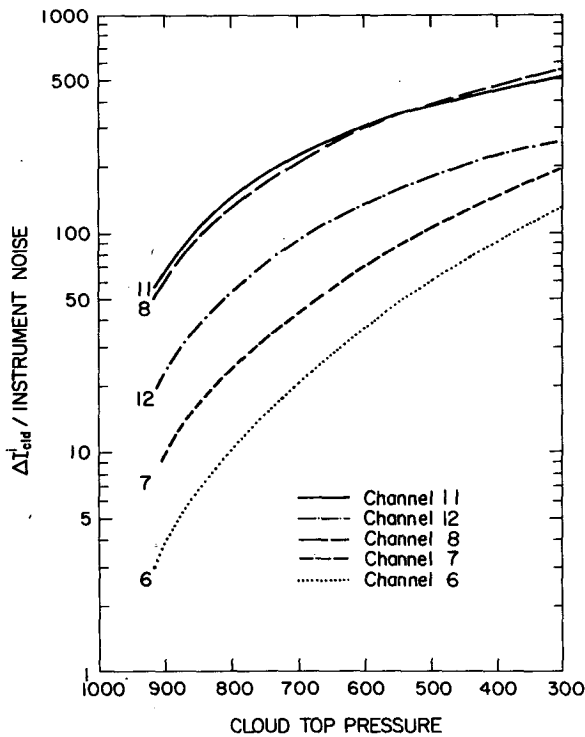


FIG. 4. Ratio of overcast cloud signal,  $\Delta I_{cld}^i = I_{cs}^i - I_0^i(P_c)$ , to HIRS-2 instrument noise as a function of cloud-top pressure. The ratio is calculated for the midlatitude profile and several of the channels which sound the lower levels of the atmosphere. For cloud amounts or emissivities less than 1.0, the signal-to-noise ratio is reduced by the factor  $\epsilon A_c$ .

The resulting rms error about the biased mean becomes

$$\sigma_P(P_c, A_c) = [Y2 - (Y1)^2]^{1/2}. \quad (15)$$

Fig. 5b shows the bias errors for 6/7 predicted from (14) and satisfactorily explains those shown in Fig. 5a. Predicted rms errors from (15) are not shown, but they explain equally well those shown in Fig. 3a. The statistical model also works well for the other two-channel combinations.

We conclude that cloud retrieval bias errors are significant and that they are caused by the nonlinear boundary constraints placed on retrieved cloud quantities.

Three simple modifications of the boundary constraints are made in order to reduce these bias errors. First, if  $(I_{cs}^i - \bar{I}^i)$  is less than the instrument noise,  $\hat{G}^{ij}$  is the ratio of Gaussian noise and will range from  $-\infty$  to  $+\infty$ . Many of these cases will be retrieved as cloud at the tropopause ( $\hat{G}^{ij} \approx 1$ ). Low clouds and clear-sky conditions will both be biased toward high-cloud retrievals. In order to discriminate against this occurrence, we specify clear-sky conditions if  $\Delta \bar{I}_{cld}^i$  is less than twice the instrument noise.

Second,  $G^{ij}(P_c)$  is independent of cloud amount. If  $\hat{G}^{ij}$  indicates a cloud too low, Eq. (3) might give  $\hat{A}_c > 1.0$ . If cloud amount is simply truncated to 1.0, an inconsistency will exist between the measured radiance and the radiance calculated using the retrieved  $\bar{P}_c$  and  $\hat{A}_c = 1.0$ . In this case we treat the

measured radiance in the lowest sounding channel  $j$  as a direct estimate of  $I_j^0(P_c)$ . In the presence of profile information  $I_j^0$  is a known monotonic function of  $P_c$ . The new cloud pressure and amount will be consistent with the measured radiance. Note that this problem does not occur for the Chahine method be-

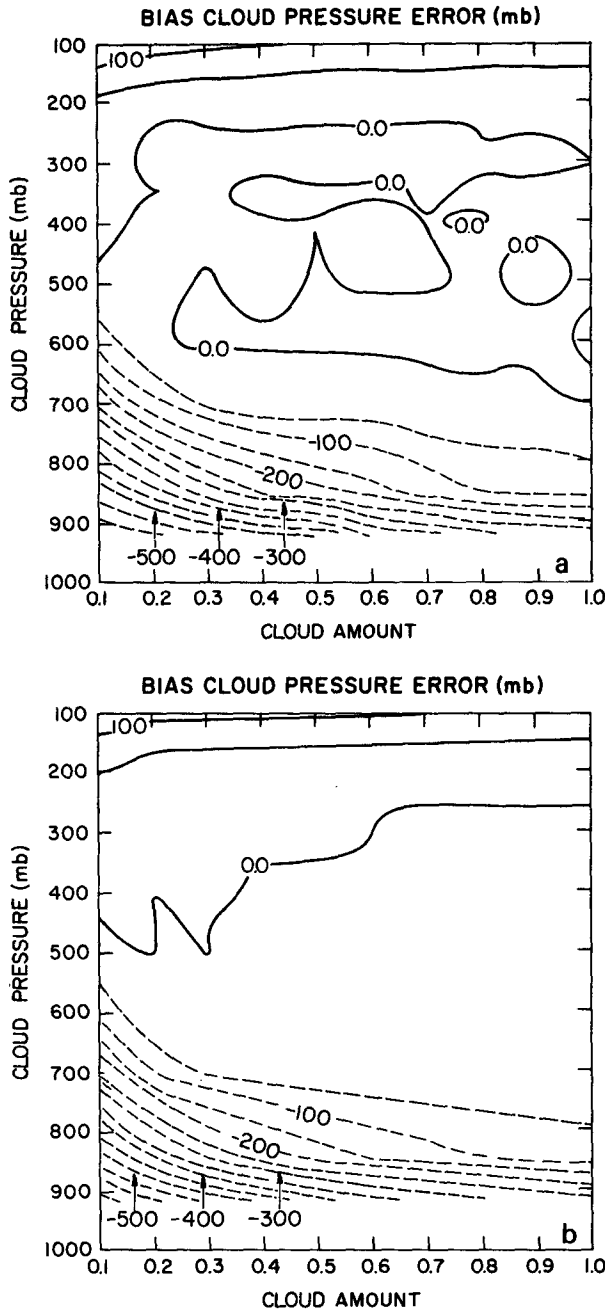


FIG. 5. Bias error of mean retrieval cloud-top pressure (retrieved - actual) for the midlatitude profile using channel combination 6/7. The error source is instrument noise. Bias error using the radiance-ratioing method is shown in (a). Bias error predicted using the Gaussian model [Eq. (14)] are shown in (b). Contour interval is 50 mb.

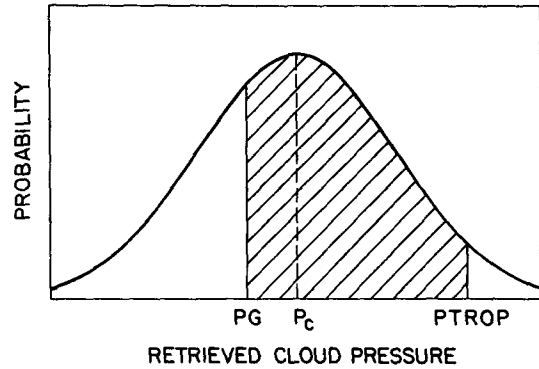


FIG. 6. An idealized probability distribution of retrieved cloud-top pressure for an actual cloud pressure  $P_c$ .  $P_G$  and  $P_{TROP}$  are physical limits for allowable retrieved cloud pressures, i.e.,  $P_G \approx$  surface pressure and  $P_{TROP} \approx$  tropopause pressure. The figure shows the inconsistency between the actual cloud-top pressure and the mean of retrieved cloud-top pressures.

cause the difference between measured and calculated radiances is minimized. With this boundary condition modification, the Chahine and radiance-ratioing methods give similar rms and bias errors (differences  $< 10\%$ ) for two-channel retrievals.

Third, much of the low-cloud bias is caused by the retrieval of clear-sky conditions when low clouds are actually present in the field of view. Since low clouds appear bright in the visible channel, we can often alleviate this problem for daytime retrievals. If we allow the visible channel to give us a simple cloud/no-cloud decision, the impact of the lower boundary condition can be reduced. For example, when the visible channel indicates cloud but the infrared channels indicate clear sky, we set  $P_c = 920$  mb.

From the above considerations, we identify two distinct cloud retrieval situations. To evaluate cloud retrieval at night, only the first two boundary condition modifications are incorporated. Cloud pressure bias errors for 6/7 night retrievals are shown in Fig. 7a. Low-cloud bias errors are significantly lower than in Fig. 5a, but are still rather large. For daytime cloud retrievals we assume our test clouds are all detected in the visible channel and include modification three. Cloud-pressure bias errors for 6/7 daytime retrievals are shown in Fig. 7b. Low-cloud bias errors are greatly reduced.

The boundary-condition modifications above cause only small changes in the rms cloud pressure errors shown in Fig. 3a. The largest effect is a reduction of rms errors for low clouds (below 800 mb) by 5–10%. Although not shown, we note that the instrument noise model given by (10)–(15) can be modified to include the above boundary-condition changes.

*c. Cloud-fraction rms and bias errors*

We turn now to cloud-fraction rms errors. Instrument noise is still the only source of error. Once

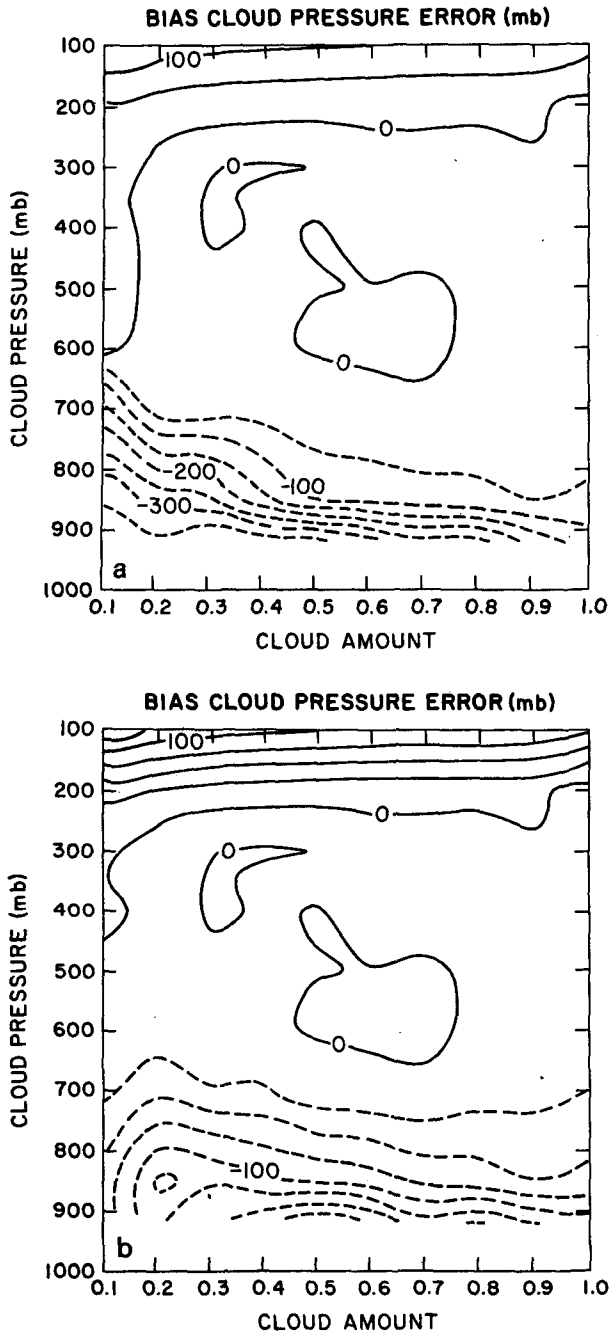


FIG. 7. Bias error of mean retrieved cloud-top pressure (mb). Retrieval conditions are the same as Fig. 5a except that boundary constraints on retrieved cloud height and cloud amount are modified to those typical of night retrieval (see text) in (a) and day retrieval in (b). Contour interval is 50 mb in (a) and 25 mb in (b).

cloud pressure has been determined, cloud amount is found from the lowest sounding channel  $j$  using (3). For black clouds the amount is given by

$$\begin{aligned} \bar{A}_c &= A_c + \delta A_c \\ &= \frac{(I^j + \delta I^j) - I_{cs}^j}{[I_0^j(P_c) + \delta I_0^j(\delta P_c)] - I_{cs}^j} \end{aligned} \quad (16)$$

It can be shown that  $\delta I_0^j(\delta P_c)/\delta I^j \gg 1$ , i.e., errors in the calculation of overcast radiances due to cloud-pressure errors are much larger than instrument noise errors. The ratio increases from a minimum of  $4/A_c$  ( $P_c = 200$  mb) to approximately  $20/A_c$  ( $P_c = 920$  mb). This magnification is a consequence of obtaining  $P_c$  from  $G^{ij}(P_c)$ . As a result, the errors in  $I_0(\bar{P}_c)$  are only indirectly related to the errors in the measured radiances.

Since  $\delta I_0^j(\delta P_c)$  is the dominant error in (16), cloud-pressure and fractional-coverage errors are strongly correlated. If cloud height is estimated too high, Eq. (16) indicates that cloud amount will be estimated too low. The reverse situation also is true. Using the above result, we relate cloud-fraction errors to cloud-pressure errors by expanding (16) to obtain (for unbiased errors)

$$\sigma_A(P_c, A_c) = A_c \left[ \frac{\delta I_0^j[\sigma_P(P_c, A_c)]}{I_0^j(P_c) - I_{cs}^j} \right] \quad (17)$$

Cloud-amount bias error can be predicted by the same method used for cloud-pressure bias error.

Fig. 8a shows rms cloud fraction errors obtained by using 6/7 for daytime boundary conditions. The decrease of rms error toward the surface is caused by the surface cloud boundary. We see that the errors do not increase rapidly as  $A_c \rightarrow 0$ , as we noted for cloud-pressure rms errors. This is predicted by (17), since  $\sigma_P$  and  $A_c$  are inversely related.

Bias cloud amount errors for 6/7 (daytime) are shown in Fig. 8b. For the lowest cloud levels, cloud amounts are biased low due to the previously mentioned bias toward high-cloud heights. Above this level we find bias errors affected by physical limits on cloud amounts analogous to the previously discussed limits for cloud pressures. Low-cloud amounts are biased too high, and cloud amounts near 1.0 are biased too low.

Since cloud amount errors can be effectively predicted from a knowledge of cloud pressure errors, the following section of the paper will concentrate on cloud pressure error results.

### 5. Errors due to uncertainties in temperature profiles and water vapor profiles

The cloud retrieval methods under study must specify clear-sky radiances  $I_{cs}^i$  and overcast radiances  $I_0^i(P_c)$  before cloud properties can be retrieved. These radiances were known exactly for our previous instrument noise analysis. We now consider the cloud-retrieval error caused by uncertainties in  $I_0^i(P_c)$  and  $I_{cs}^i$ . Two retrieval situations are identified and considered.

First, it might be possible to directly measure clear-sky radiances in a FOV near the cloud under study (Smith and Platt, 1978). By "near" we mean that the same temperature and water vapor profiles (which determine  $I_{cs}^i$ ) occur in both the cloudy and



clear fields of view. Since we cannot measure  $I_0(P_c)$  directly, we calculate this quantity from some imperfect knowledge of the temperature and water vapor profiles using (2).

Second, our nearest measured clear-sky radiances may not be representative of the atmospheric conditions for the cloud we wish to retrieve. For example, clouds in large storm systems might be several hundred kilometers from the nearest clear area. Near storm fronts, atmospheric conditions vary rapidly between clear and cloudy areas. In these cases temperature and water vapor profile errors will be present in estimated  $I_{cs}^i$ , whether the radiances are measured or calculated.

We evaluate errors due to profile uncertainties for the same conditions that were considered for instrument noise. Temperature errors [affecting the Planck functions  $B(\nu^i, T)$  and to a lesser extent the weighting functions  $d\tau^i/d \ln P$ ] and water vapor errors [affecting only the weighting functions  $d\tau^i/d \ln P$ ] are Gaussian with zero mean. They are specified independently for each model level. Water vapor errors are given as a percent of the correct mixing ratio at any level. To isolate the effect of profile uncertainties, instrument noise is set to zero. One modification must be made to the boundary conditions used earlier. In the instrument noise case we assumed clear skies existed when  $\Delta \bar{I}_{\text{cld}} < 2$  times the instrument noise. The use of such a filter depends on two assumptions: that the noise in the two channels used to determine  $\hat{G}^{\text{cl}}$  is uncorrelated, and that the magnitude of the noise can be specified beforehand. Neither of these assumptions is satisfied in the case of profile uncertainties. Therefore, we replace the condition on  $\Delta \bar{I}_{\text{cld}}$  with a condition on the measured estimate of the cloud functional  $\hat{G}^{\text{cl}}$ . If  $\hat{G}^{\text{cl}} < G$  (920 mb) or  $\hat{G}^{\text{cl}} > 1.2$ , we assume clear-sky conditions. If  $G(\text{PTROP}) < \hat{G}^{\text{cl}} < 1.2$ , we set  $P_c = \text{PTROP}$ . The limit of 1.2 is chosen because rms  $P_c$  errors for clouds near the tropopause indicate that  $\hat{G}^{\text{cl}}$  will not exceed 1.2 for a reasonable range of profile uncertainties (rms temperature noise  $\leq 5^\circ\text{C}$ , rms water vapor noise  $\leq 100\%$ ). A value of  $\hat{G}^{\text{cl}} > 1.2$  therefore indicates low-cloud (day retrieval) or clear skies (night retrieval).

We first consider profile errors in  $I_0(P_c)$ ,  $I_{cs}$  and  $I$  are known exactly. In this case the "measured"  $G^{\text{cl}}$  from (5) is also known exactly. The only error in calculating  $P_c$  is the uncertainty in the  $G^{\text{cl}}(P_c)$  calculated from (6). We noted in Fig. 2 that  $G^{\text{cl}}(P_c)$  varied only slightly between mean midlatitude and tropical profiles. We might expect that random profile uncertainties will produce only small errors.

Taking as an example rms temperature noise of  $2.0^\circ\text{C}$  and water vapor mixing ratio noise of 50% (midlatitude profile), we find rms  $P_c$  errors of 25 mb with bias errors  $< 5$  mb. These errors are independent of cloud amount because the calculated  $G^{\text{cl}}(P_c)$  is independent of cloud amount. In addition, the

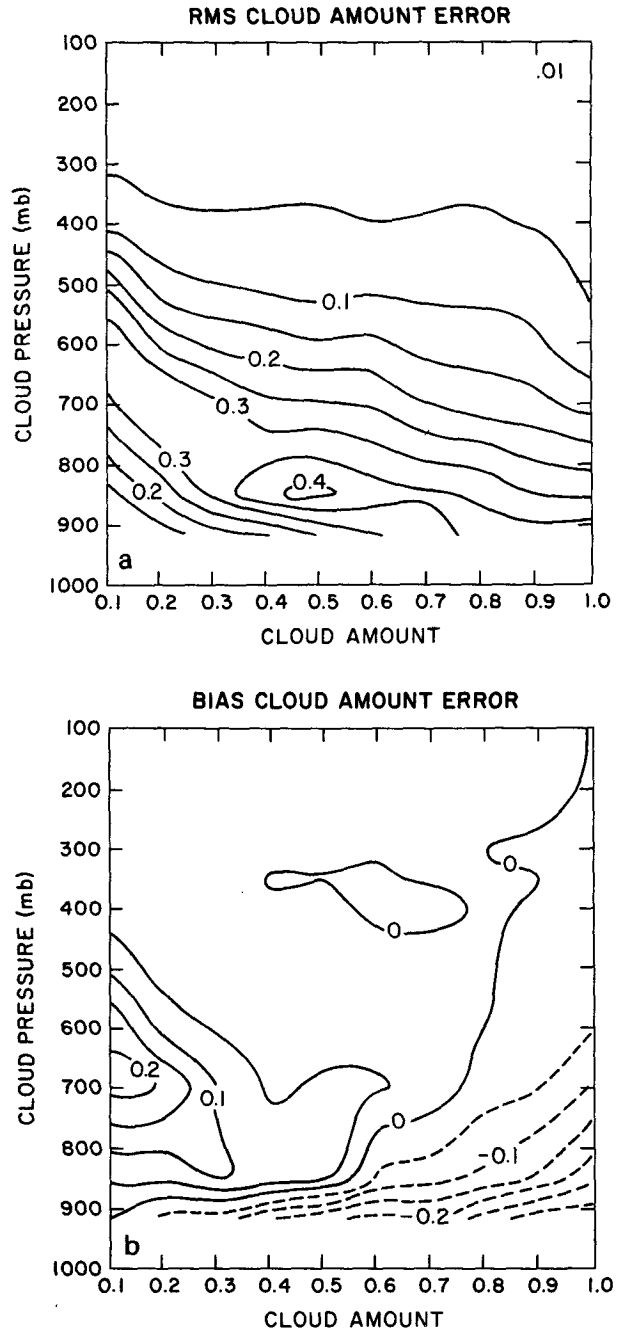


FIG. 8. Standard deviation (a) and bias (b) of retrieved cloud-amount error caused by instrument noise. Errors are shown using channel combination 6/7, the midlatitude profile, and daytime cloud-boundary constraints. Contour interval is 0.05.

errors are approximately independent of cloud height. The retrieval errors are therefore independent of cloud signal  $\Delta I_{\text{cld}}$ . Consistent with this result, channel combinations 6/7, 5/7, 4/7, 7/8, 6/8, 12/11, 13/11 and 14/11 all give similar errors. A separate analysis of temperature and water vapor profile errors shows that for our test case, temperature error dominates the retrieval error. For purposes of extrapolation,

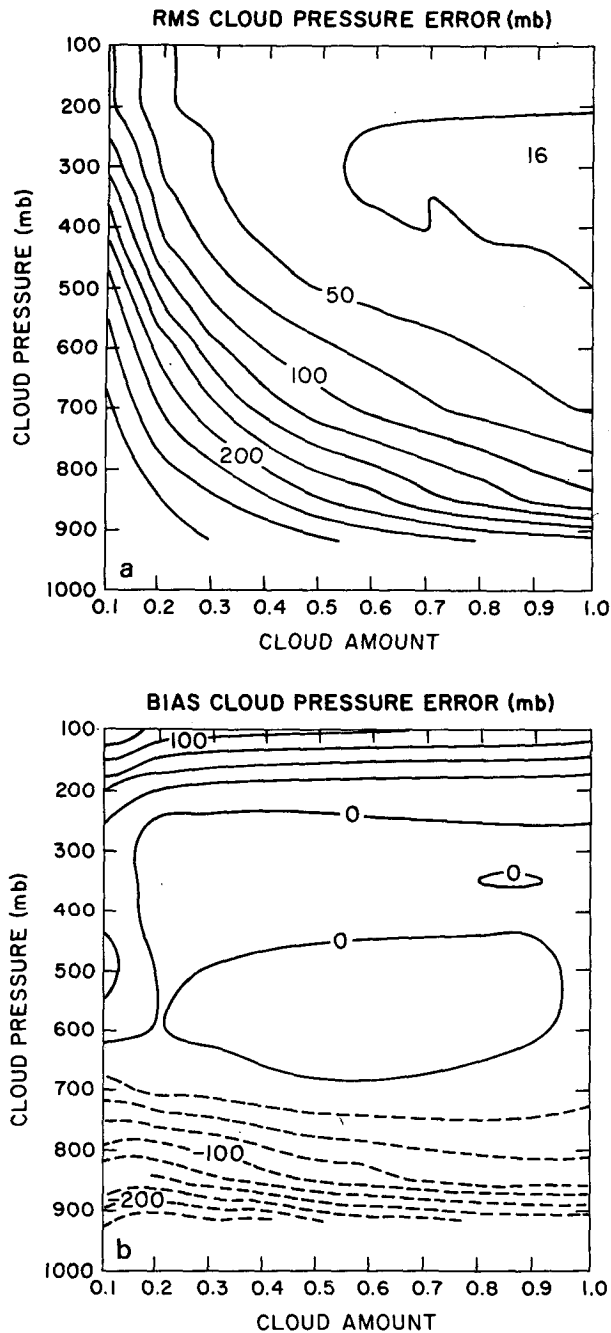


FIG. 9. Standard deviation (a) and bias (b) of retrieved cloud-top pressure error (mb) caused by an rms temperature profile noise of  $2.0^{\circ}\text{C}$ , and a water vapor profile noise of 50%. Errors are shown using channel combination 6/7, the midlatitude profile, and daytime cloud boundary constraints. Contour intervals are 25 mb.

retrieval error is linearly proportional to temperature error. We conclude that errors in  $G^{\text{tr}}(P_c)$  due to uncertainty in  $I_0(P_c)$  are likely to be insignificant compared to instrument noise errors, especially for low clouds.

We now consider profile errors in both  $I_0(P_c)$  and

$I_{cs}$ . In this case error occurs in both the calculated  $G^{\text{tr}}(P_c)$  and the measured  $\hat{G}^{\text{tr}}$ .

Figs. 9a and 9b show midlatitude rms and bias cloud-pressure errors for the 6/7 channel combination with  $2.0^{\circ}\text{C}$  temperature noise and 50% water vapor noise. The results are for daytime boundary conditions. As with instrument noise, the errors are strongly related to the cloud signal  $\Delta I_{\text{cld}}$ . Small cloud amounts or low cloud heights lead to large retrieval errors. Comparing to Figs. 3a and 7b, we see that the rms and bias errors are slightly larger than those for instrument noise. The lowest sounding channels again gave the smallest errors, but errors for 6/7, 12/11 and 7/8 are all similar in magnitude (within 10–50%). For instrument noise this was not true because the ratio of instrument noise to cloud signal  $\Delta I_{\text{cld}}$  varied for different spectral regions. For temperature errors the noise is proportional to  $(dB/dT)\delta T$ . The signal  $\Delta I_{\text{cld}}$  is proportional to  $(dB/dT)(T_G - T_c)$ . The signal-to-noise ratio is then proportional to  $\delta T/(T_G - T_c)$ , which is independent of spectral interval. As with instrument noise, the use of all four channels within a spectral region ( $4.3\text{--}15\ \mu\text{m}$ ) slightly increases errors for clouds below 500 mb and decreases the error above 500 mb. At 200 mb, four-channel errors are  $\sim 30\%$  smaller than those of the two-channel solutions.

A separate analysis of temperature and water vapor errors again shows that for the assumed profile errors, the temperature errors dominate and that the retrieval errors are linear functions of the temperature error. This linearity will not apply, however, for errors near the surface and tropopause boundaries.

We conclude that errors in  $I_{cs}$  can cause large cloud retrieval errors. Three methods have been proposed to circumvent these errors. First, clear-sky radiances might be directly measured near the cloud to be retrieved. Second, two FOV's with the same cloud-height and clear-sky radiances but differing cloud amounts can be used to eliminate the effects of clouds on the radiances and thereby obtain an estimate of clear-sky radiances (Smith and Wolf, 1976; Chahine, 1974; Smith, 1968). This method is used operationally for the HIRS-2 data from TIROS-N and is called the  $N^*$  approach. Third, for the same conditions as the  $N^*$  approach, a direct estimate of  $\hat{G}^{\text{tr}}$  may be made by ratioing the radiance difference between two fields of view, i.e.,  $\hat{G}^{\text{tr}} = (I_1^i - I_2^i)/(I_1^c - I_2^c)$  without directly defining  $I_{cs}$  (McCleese and Wilson, 1976). Clear-sky radiance still must be estimated, however, in order to retrieve cloud amounts. A recent test of the operational TIROS-N temperature soundings (Phillips *et al.*, 1979) provides a rough idea of how often errors in  $I_{cs}$  will be important. Clear-sky radiances (and temperature profiles) were determined for 600 "boxes" ( $250\ \text{km} \times 250\ \text{km}$ ) between  $30\text{--}60^{\circ}\text{N}$  over a 9-day period. Of these 600 sample boxes, 39% were too overcast

for either direct measurement of clear-sky radiances or use of the  $N^*$  approach. We tentatively conclude that errors in  $I_{cs}$  will be important for a large portion of the earth's cloudiness. For these areas  $I_{cs}$  estimates might utilize either NMC analyses or microwave profile retrievals. rms temperature errors might range from 1 to 5°C. For channel combinations 12/11 retrieval errors due to profile uncertainty become larger than errors due to instrument noise for temperature rms errors  $\geq 0.5^\circ\text{C}$ . For 8/7 the threshold is  $\approx 0.8^\circ\text{C}$ . For 6/7 the threshold is  $\approx 1.5^\circ\text{C}$ . For rms temperature errors much greater than  $2^\circ\text{C}$ , temperature errors will dominate and all three channel combinations will give similar errors for most clouds. In the case of high clouds for  $\epsilon A_c < 0.2$ , the  $4.3 \mu\text{m}$  channels show higher errors due to their low sensitivity at the low temperatures typical of high clouds. The  $15 \mu\text{m}$  channels should be used.

## 6. Comparison to previous results

Chahine (1975) reported typical errors of 0.05 in cloud amount and 25 mb in cloud top pressure. Four tropospheric sounding  $15 \mu\text{m}$  channels, similar to those on the HIRS instrument, were used with his method. A systematic error of 2% in the weighting function  $d\tau/d \ln P$  and a uniformly distributed instrument noise of  $0.25 \text{ mW m}^{-2} \text{ sr}^{-1} \text{ cm}$  (maximum) were used. These errors are approximately equivalent to a Gaussian rms value of  $0.15 \text{ mW m}^{-2} \text{ sr}^{-1} \text{ cm}$ . Considering only instrument noise effects, our results indicate errors of 25 mb and 0.05, only for cloud pressures less than 600 mb with minimum cloud amount depending on the height considered. For example, at 500 mb cloud amount must be greater than 0.5 to reach these error limits. Seemingly, the errors quoted by Chahine were derived from test cases of clouds above 500 mb.

Smith and Platt (1978, hereafter referred to as SP) compared satellite-derived cloud heights to ground-based lidar determinations. Clear FOV's were chosen for representative clear-sky radiance measurements made with the Nimbus 5 ITPR (Infrared Temperature Profile Radiometer) instrument. Nearby radiosonde profiles served to define  $G(P_c)$  for the radiance-ratioing method as previously described. Channels equivalent to 5/7 were used for clouds above 500 mb and the 7/8 combination for clouds at or below 500 mb (as determined by 5/7). Clouds below 500 mb are assumed black. Assuming that the only error is due to instrument noise in the measurement of clear and cloudy radiances, we construct a noise analysis similar to that in Section 3. The resulting errors are approximately  $\sqrt{2}$  larger than those obtained with noise-free clear-sky radiances. Table 1 presents the results from SP along with the rms and bias pressure errors from the present noise analysis. The errors quoted are for Nimbus

TABLE 1. The first four columns show the results of Smith and Platt (1978) comparing ITPR sounder retrieved cloud-top pressures with lidar and radiosonde estimated cloud-top pressures. ITPR derived cloud amounts are also given. The final two columns give rms and bias cloud-top pressure errors from the present analysis assuming a cloud pressure and amount equal to that retrieved by Smith and Platt.

Radiosonde pressure (mb)	Lidar pressure	ITPR		Present study rms $P_c$ (mb)	Retrieved actual bias $P_c$ (mb)
		Pressure	Amount		
420 (?)	440	450	0.30	55	-0
830	830	800	0.39	80	-10
700 (?)	630	600	0.13	110	-0
400	420 (?)	450	0.24	70	-0
460 (?)	—	400	1.00	10	-0
330	—	300	0.80	10	-0
850	830	850	0.25	135	-45
500	800 (?)	500	0.14	80	-0
550	550	550	0.65	20	-0

5 ITPR instrument noise levels. A midlatitude profile is assumed.

Question marks denote that only weak lidar returns were obtained from the cloud tops. Radiosonde cloud pressures were estimated from the relative humidity profile. The questionable estimates were noted by SP. In general, the ITPR cloud-pressure agreement appears to be better than it should, especially for low clouds. The sample, however, is small and cloud pressure was selected by SP to give the best agreement between the lidar and the 3-4 surrounding ITPR cloud retrievals.

Smith and Woolf (1976, hereafter referred to as SW) reported cloud top pressure errors for a statistical eigenfunction fit of nine  $G^{\hat{u}}(P_c)$  ratios using Nimbus 6 channel combinations. Channel pairs were chosen in the  $15$  and  $4.3 \mu\text{m}$  regions such that  $\epsilon^i = \epsilon^j$ . The theoretical analysis assumed that clear sky radiances were known but that atmospheric profile information was not given. This is equivalent to our previous analysis for profile uncertainties with known clear-sky radiances. Boundary conditions were similar to our daytime retrieval conditions. SW found that errors without instrument noise were approximately independent of  $P_c$  and  $A_c$ , in agreement with our results in Section 5. Their cloud-pressure rms errors, averaged over a range of test cloud heights and atmospheric profiles (100 samples) were 32 mb for tropical conditions and 46 mb for midlatitude conditions. For comparison, using our analysis with the four  $15 \mu\text{m}$  channels we find errors similar to SW for temperature noise of  $4^\circ\text{C}$  and water vapor noise of 75%.

The SW analysis then added instrument noise to the "measured" radiances and the same samples (100 each) were performed for a range of cloud amounts from 0.1 to 1.0. Their total rms cloud pressure errors are shown by a solid line in Fig. 10. The errors are averaged over a range of cloud heights

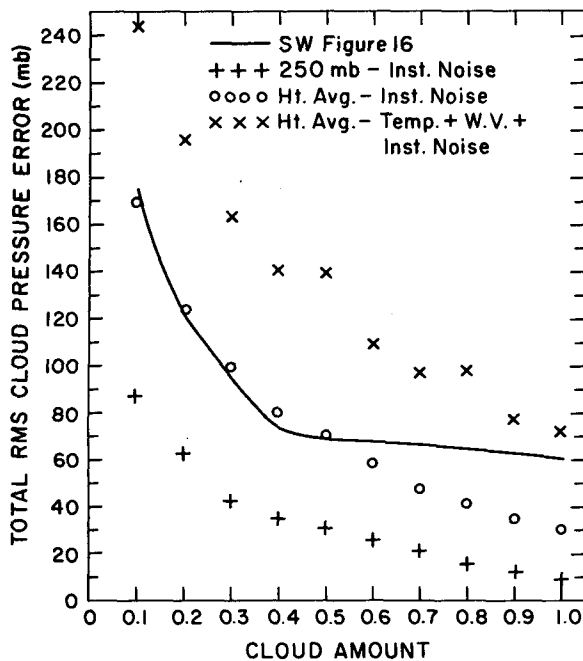


FIG. 10. Total rms cloud-top pressure error (includes bias error) as a function of cloud amount. Results for the present analysis are compared to those of Smith and Woolf (1976). Retrieval conditions and error sources are described in Section 6 of the text.

for midlatitude conditions. SW conclude that instrument noise errors dominate for  $A_c < 0.4$ . For comparison, we averaged our instrument noise results (daytime boundary conditions) over the cloud heights used by SW. An average of our results for 6/7 and 12/11 produces the circles in Fig. 10. This comparison indicates that the eigenfunction analysis probably weighted the 15 and 4.3  $\mu\text{m}$   $G^u$  values similarly. Since the eigenfunctions were fit to minimize retrieval errors caused by uncertainties in  $I_0(P_c)$  [or  $G^u(P_c)$ ], this is a reasonable conclusion because errors due to uncertainties in  $I_0(P_c)$  are approximately independent of channel combination.

The height-averaged errors shown by SW can be misleading. Instrument noise errors vary by an order of magnitude as a function of cloud height. Height-averaged errors will be dominated by low-level cloud errors. The crosses in Fig. 10 show our instrument noise results for midlatitude clouds at 250 mb. For high clouds we would conclude that instrument noise errors dominate for  $A_c < 0.2$ . For clouds at 850 mb instrument noise errors would dominate for all cloud amounts. Care should be taken to recognize the large variation of cloud retrieval errors as a function of both cloud amount and cloud height.

Finally, we compare our results for profile uncertainties in clear sky radiances with the SW results. Cloud retrieval errors are calculated for 6/7 using midlatitude daytime conditions with instrument noise, temperature noise of 2.0°C, and water vapor

noise of 50%. The results are indicated with an  $\times$  in Fig. 10, averaged over the SW cloud heights. Errors in clear sky radiances will dominate the previously reported errors for small profile uncertainties.

## 7. Conclusions

We present a brief summary of the major results of the analysis:

1) The Chahine and radiance-ratioing retrieval methods are equivalent for two-channel cloud retrievals.

2) The two lowest sounding channels provide the majority of cloud information. The addition of channels sounding the upper tropospheric levels, however, can reduce high-cloud errors by as much as one-third.

3) Cloud retrieval errors are a strong function of both the cloud amount and the cloud height within the satellites field of view. The largest errors occur for low-cloud amounts and low-cloud heights.

4) Significant bias errors are noted for retrieved cloud-top pressures and amounts. These biases occur predominantly for low clouds and are shown to result from the application of physical constraints on retrieved cloud properties [ $0.0 \leq A_c \leq 1.0$ ,  $P(\text{ground}) \leq P_c \leq P(\text{tropopause})$ ]

5) Optimal channel selection varies for different error sources. For instrument noise, use of the 4.3 and 11  $\mu\text{m}$  channels provide the smallest errors. For profile uncertainties affecting clear sky radiances, the 15  $\mu\text{m}$  channels generally produce smaller errors.

6) Cloud retrieval errors caused by uncertainties in clear-sky radiances can be large. Errors due to a temperature profile uncertainty of 2°C will dominate instrument noise errors for all cloud amounts and heights, independent of the retrieval channels used. Errors due to water vapor profile uncertainties are much smaller.

In the event that retrieval error sources can be limited to instrument noise, infrared sounder cloud retrieval is feasible for most cloud heights and amounts. Small amounts of low cloud ( $850 \text{ mb}$ ,  $A_c \leq 0.3$ ), however, are poorly retrieved even for the instrument noise case. More commonly, we expect substantial errors in estimated clear sky radiances, causing large cloud-height and cloud-amount errors for low clouds ( $850 \text{ mb}$ , all cloud amounts). Most middle- and high-level clouds are still retrieved faithfully.

## REFERENCES

- Cess, R. D., 1974: Radiative transfer due to atmospheric water vapor: Global consideration of the earth's energy balance. *J. Quant. Spectros. Radiat. Transfer*, **14**, 861–871.
- Chahine, M. T., 1974: Remote sounding of cloudy atmospheres. I. The single cloud layer. *J. Atmos. Sci.*, **31**, 233–243.

- , 1975: An analytical transformation for remote sensing of clear-column atmospheric temperature profiles. *J. Atmos. Sci.*, **32**, 1946–1952.
- Fels, S. B., and M. D. Schwarzkopf, 1975: The simplified exchange approximation: A new method for radiative transfer calculations. *J. Atmos. Sci.*, **32**, 1475–1488.
- McCleese, D. J., and L. S. Wilson, 1976: Cloud top heights from temperature sounding instruments. *Quart. J. Roy. Meteor. Soc.*, **102**, 781–790.
- Phillips, N., L. McMillan, A. Gruber and D. Wark, 1979: An evaluation of early operational temperature soundings from TIROS-N. *Bull. Amer. Meteor. Soc.*, **60**, 1188–1197.
- Platt, C. M. R., and A. C. Dille, 1979: Remote sounding of high clouds: II. Emissivity of cirrostratus. *J. Appl. Meteor.*, **18**, 1144–1150.
- Schneider, S. H., 1972: Cloudiness as a global climatic feedback mechanism: The effects on the radiation balance and surface temperature of variations in cloudiness. *J. Atmos. Sci.*, **29**, 1413–1422.
- Smith, W. L., 1968: An improved method for calculating tropospheric temperature and moisture from satellite radiometer measurements. *Mon. Wea. Rev.*, **96**, 387–396.
- , and H. M. Woolf, 1976: The use of eigenvectors of statistical covariance matrices for interpreting satellite sounding radiometer observations. *J. Atmos. Sci.*, **33**, 1127–1140.
- , and C. M. R. Platt, 1978: Comparison of satellite-deduced cloud heights with indications from radiosonde and ground-based laser measurements. *J. Appl. Meteor.*, **17**, 1796–1802.
- , H. M. Woolf and W. J. Jacob, 1970: A regression method for obtaining real-time temperature and geopotential height profiles from satellite spectrometer measurements and its application to Nimbus 3 SIRS observations. *Mon. Wea. Rev.*, **98**, 604–611.
- Stephens, G. L., and P. J. Webster, 1979: Sensitivity of radiative forcing to variable cloud and moisture. *J. Atmos. Sci.*, **36**, 1450–1466.